

Review

A Review of Treatment Techniques for Short-Chain Perfluoroalkyl Substances

Yang Liu ^{1,*}, Tingyu Li ¹, Jia Bao ^{1,*}, Xiaomin Hu ², Xin Zhao ², Lixin Shao ¹, Chenglong Li ¹ and Mengyuan Lu ¹

¹ School of Environmental and Chemical Engineering, Shenyang University of Technology, Shenyang 110870, China; LITingyu990109@163.com (T.L.); shaolixin0503@163.com (L.S.); lcl960315@163.com (C.L.); lumengyuan2022@163.com (M.L.)

² School of Resources and Civil Engineering, Northeastern University, Shenyang 110819, China; hxmin_jj@163.com (X.H.); zhaoxin@mail.neu.edu.cn (X.Z.)

* Correspondence: liuyang@sut.edu.cn (Y.L.); baojia@sut.edu.cn (J.B.)

Abstract: In recent years, an increasing amount of short-chain perfluoroalkyl substance (PFAS) alternatives has been used in industrial and commercial products. However, short-chain PFASs remain persistent, potentially toxic, and extremely mobile, posing potential threats to human health because of their widespread pollution and accumulation in the water cycle. This study systematically summarized the removal effect, operation conditions, treating time, and removal mechanism of various low carbon treatment techniques for short-chain PFASs, involving adsorption, advanced oxidation, and other practices. By the comparison of applicability, pros, and cons, as well as bottlenecks and development trends, the most widely used and effective method was adsorption, which could eliminate short-chain PFASs with a broad range of concentrations and meet the low-carbon policy, although the adsorbent regeneration was undesirable. In addition, advanced oxidation techniques could degrade short-chain PFASs with low energy consumption but unsatisfied mineralization rates. Therefore, combined with the actual situation, it is urgent to enhance and upgrade the water treatment techniques to improve the treatment efficiency of short-chain PFASs, for providing a scientific basis for the effective treatment of PFASs pollution in water bodies globally.

Keywords: low carbon; short-chain PFASs; water treatment; adsorption; advanced oxidation



Citation: Liu, Y.; Li, T.; Bao, J.; Hu, X.; Zhao, X.; Shao, L.; Li, C.; Lu, M. A Review of Treatment Techniques for Short-Chain Perfluoroalkyl Substances. *Appl. Sci.* **2022**, *12*, 1941. <https://doi.org/10.3390/app12041941>

Academic Editor: Dino Musmarra

Received: 18 January 2022

Accepted: 9 February 2022

Published: 12 February 2022

Publisher's Note: MDPI stays neutral with regard to jurisdictional claims in published maps and institutional affiliations.



Copyright: © 2022 by the authors. Licensee MDPI, Basel, Switzerland. This article is an open access article distributed under the terms and conditions of the Creative Commons Attribution (CC BY) license (<https://creativecommons.org/licenses/by/4.0/>).

1. Introduction

Since the 1950s, perfluoroalkyl substances (PFASs) have been widely used in industrial production and commercial products, involving chrome plating, foam extinguishing agents, aviation hydraulic oil, and food packaging paper [1,2]. They are a class of man-made chemicals with all the hydrogen atoms on the carbon skeleton replaced by fluorine atoms, together with a terminal functional group [3]. Abbreviations for different PFASs are shown in Table 1. Due to the strong energy of the C–F bond (536 kJ/mol), PFASs possess exclusive physio-chemical characteristics, including environmental persistence, extraordinary resistance to both environmental and biological degradation, high thermal and chemical stability against oxidation, photolysis, and hydrolysis reactions, hydrophobicity and oleophobicity, as well as multiple toxicities [4]. Moreover, many PFAS (precursors) can easily degrade into persistent PFAS (acids). Therefore, long-chain PFASs (C8–C14) and their sodium, as well as ammonium, salts were added into the candidate list of regulatory substances in the EU, and PFOA and PFOS were added in the Stockholm Convention on Persistent Organic Pollutants (POPs) list [5]. With the ban of long-chain PFASs, short-chain PFASs (PFCAs < C8, PFSAs < C7) have been produced and used as substitutes in large quantities.

With the improvement of modern analytical techniques such as high-resolution mass spectrometry in non-target and suspect screening approaches in recent years, the researchers

found that long-chain PFASs tended to be adsorbed by solid matter (soil, sediment, etc.), which made them less mobile. However, short-chain PFASs showed a high polarity and solubility, which rendered them difficult to be removed through environmental adsorption and water treatment processes, thus contributing to long-term mobility in the water cycle through migration of surface water, groundwater, and natural and urban water systems [6–9]. However, short-chain PFASs show similar properties with long-chain congeners, including being persistent, bioaccumulative, and toxic to a certain extent [10]. Therefore, short-chain PFASs could be classified as persistent and mobile organic compounds (PMOCs) [6].

Table 1. Abbreviation for different PFASs.

Abbreviation			
TFA	Trifluoroacetic acid	GenX	2,3,3,3-Tetrafluoro-2-(1,1,2,2,3,3,3-heptafluoropropoxy) propanoic acid
PFSAs	Perfluoroalkane sulfonates	PFCAAs	Perfluoroalkyl carboxylic acids
PFBS	Perfluorobutane sulfonic acid	PFBA	Perfluorobutanoic acid
PFPrA	Pentafluoropropionic acid	PFPeA	Perfluoropentanoic acid
PFHxS	Perfluorohexane sulfonic acid	PFHxA	Perfluorohexanoic acid
PFOS	Perfluorooctane sulfonic acid	PFOA	Perfluorooctanoic acid
PFHpA	Perfluoroheptanoic acid	PFNA	Perfluorononanoic acid
PFDA	Perfluorodecanoic acid	PFDoA	Perfluorododecanoic acid

Large quantity usage of short-chain PFASs could lead to accumulation in the water cycle and water pollution, thereafter threatening drinking water quality. For instance, the concentrations of PFBS and PFBA in Tangxun Lake of Wuhan in China reach up to 3.66 µg/L and 4.77 µg/L, respectively [11]. There was a serious PFBS contamination in groundwater around fluorochemical plants in Fuxin in China, with a concentration up to 31 µg/L [12], exceeding 10 times the health risk limits (HRLs) in drinking water (3 µg/L) issued by the Minnesota Department of Health (MDH). Thus, it is an urgent incident to effectively develop suitable water treatment techniques to regulate short-chain PFAS contaminations in waters.

At present, activated carbon (AC) adsorption and ozonation are the commonly applied techniques for organic contaminant elimination in drinking water treatment. However, AC presented low efficiency for very polar compounds [6]. Meanwhile, ozonation generally exhibited poor reactive activity to polar compounds containing acidic functional groups [13], which might be a source of smaller and more polar by-products than the parent compounds [14]. Consequently, the removal efficiency of conventional treatment for short-chain PFASs was undesirable. Moreover, various techniques presented different removal efficiencies for short-chain PFASs, even requiring high energy consumption, strict operating conditions, and releasing a large number of by-pollutants [15].

Recently, the C40 Cities Network of 91 large cities committed to low carbon infrastructure to ensure carbon emissions peak by 2020 and almost halve by 2030 [16–18]. In 2020, China announced that it would take more aggressive policy measures to achieve peak carbon dioxide emissions by 2030 and achieve carbon neutrality by 2060 [19]. Specifically, the regulation instruments include applying forced power to administer high energy consumption and emission of pollutants [20,21]. Therefore, it is significant to explore effective low carbon treatment techniques to eliminate short-chain PFAS contaminations under convenient conditions.

This review aims to select suitable treatment techniques for short-chain PFASs. To achieve this aim, the low carbon treatment techniques for PFASs involving adsorption, electrochemical oxidation, photocatalytic oxidation, membrane separation, pyrolysis, and ultrasonic chemical degradation, and their individual removal efficiency, operating conditions, and removal mechanisms were systematically summarized. Thereafter, based upon

the characteristics of short-chain PFASs, the suitable treatment techniques were determined by the comparison of the applicability, as well as the pros and cons of various techniques. This will provide a scientific basis for the effective treatment and regulation of short-chain PFAS contaminations in different waters.

2. Methodology of Literature Sources

To obtain an overview of short-chain PFAS chemical usage, the present review initially focused on the risk profiles and risk management assessments. Reports that addressed fluorosurfactants and fluoropolymers were also involved. Literature related to certain use categories was retrieved for more information either on the substances used, or to understand why PFAS are, or were, necessary for a given use.

In addition, databases, patents, information from PFAS manufacturers, and scientific studies were examined via “Web of Science”, “PubMed”, and “CNKI”. The retrieved keywords involved but were not limited to “per- and polyfluoroalkyl substances”, “PFAS”, “PFAAs”, “short-chain PFAS”, “water treatment”, “adsorption”, “anion-exchange”, “advanced oxidation”, “persistent organic pollutant”, “emerging contaminant”, “low carbon”. The searches were not exhaustive in any of the sources described, and there are still many more reports, scientific studies, patents, safety data sheets, and databases with information on the usage of PFASs than the ones cited here [22].

3. Treatment Techniques for Short-Chain PFASs

3.1. Adsorption Technique

Low carbon technique of adsorption could remove contaminations effectively in the waters, which were widely applied in the treatment of PFASs. This technique uses a porous solid as the adsorbent to adsorb one or several contaminations in the wastewater (WW) that does not change physicochemical property, thus achieving the purification purpose [4]. The commonly used adsorption materials mainly include carbons, anion-exchange resins, flocculants, etc. The key influencing factors of adsorption efficiency involved ionic strength, pH, organic matter (OM) concentration, physicochemical properties of PFASs in solution, and adsorbent characteristics (such as particle size, porosity rate, and functional group on surface). Comparisons on the adsorption capacities of different adsorbents for short-chain PFASs are shown in Table 2.

3.1.1. Adsorption by Carbon-Based Adsorbents

AC adsorption. AC is widely used to remove contaminants in wastewater due to low cost, high efficiency, and convenient operation [4]. Ochoa-Herrera et al. adopted granular activated carbon (GAC) to adsorb PFBS, with an adsorption capacity of 98.7 mg/g [23]. Hansen et al. used GAC and powdered activated carbon (PAC) to carry out batch adsorption experiments for short-chain PFASs; PAC achieved higher removal rates within 10 min (20–40% for GAC, 60–90% for PAC) due to shorter internal diffusion distance and higher BET surface area (S_{BET}) of PAC [24]. This phenomenon demonstrated that the particle size of AC was a significant factor affecting the removal efficiency of short-chain PFASs, and smaller particle sizes presented superior removal efficiency. The effect of pore size on the removal efficiency of bamboo-derived AC (BdAC) and coal-based AC (microporous type) for PFHxA were investigated, revealing that the BdAC adsorption capacity was 13-fold lower than microporous ACs [25,26]. In addition, the GAC was explored to eliminate different carbon chain length PFASs [27], the removal efficiency of short-chain PFCAs was lower than congeners PFSAs, in which the removal rates of PFBA, PFPeA, PFHxA, and PFHpA were all below 19%, especially 10% for PFBS. Furthermore, the regeneration capacity of adsorbed AC was also inferior when eluting. Therefore, it is necessary to explore new catalysts to modify AC for promoting adsorption and regeneration capacity [1].

Biocarbon adsorption. Biocarbon is a pollution-free solid biofuel produced by pyrolysis of biomass under aerobic or anaerobic conditions, which contains abundant voids, high carbon content, and high calorific value. The nature of biocarbon is different due to

various raw materials and parameters in the production process [28]. Inyang and Dickenson [29] explored the adsorption capacity of hardwood biochar (HWC) and pinewood biochar (PWC) for PFBA and PFOA, demonstrating that the PFBA adsorption capacity was 3–4 times lower than PFOA. Meanwhile, the removal efficiency of HWC vaporized at 900 °C could be improved due to high S_{BET} . However, the batch adsorption kinetics experiments showed that the removal efficiency of GAC for PFBA was superior to HWC, indicating a low adsorption capacity of biocarbon for short-chain PFASs.

Carbon nanotube (CNTs) adsorption. CNTs have the advantages of easy reaction process control, convenient operation, and low cost of raw material. Deng et al. [30] used single-walled carbon nanotubes (SWCNT) and multi-walled carbon nanotubes (MWCNT) to remove short-chain PFASs (PFBA, PFHxA, PFHpA, PFBA, and PFBS) and long-chain PFASs (PFOA, PFHxS, and PFOS) under neutral conditions. It showed that 95% of PFOS and PFOA were removed by SWCNT within 5 h, but only 7.5% of PFBA was eliminated by SWCNT within 48 h, and PFSAs were more easily adsorbed than PFCAs. Moreover, in the comparison study of MWCNT functional groups, owing to the deprotonation that occurred on the carboxyl and hydroxyl functional groups, contributing to lower hydrophobicity and more negative surface potential, the adsorption efficiency of non-functional MWCNT for short-chain PFASs was improved. Therefore, based upon the above studies, the adsorption efficiency and technical maturity of CNTs were similar to ACs.

The main adsorption mechanism of carbon materials was hydrophobic and electrostatic effects, as well as possible hydrogen bonds and covalent bonds effects [4]. The hydrophobic effect would be improved with an increased C-F chain length; thus, long-chain PFASs were better adsorbed than short-chain congeners. Meanwhile, the removal efficiency of adsorbents for PFASs was also depended on the terminal functional groups; for instance, the removal efficiency of PFSAs was better than PFCAs. In addition, the electrostatic attraction could occur between the anionic PFASs and positive charge adsorbents. Therefore, the changes of ionic strength involving cations or anions and pH in the solution would influence the adsorption efficiency. For example, the increase of ionic strength caused by monovalent or divalent cations (Na^+ , K^+ , Ca^{2+} , etc.) might enhance PFAS removal efficiency, while the pH increase would reduce the adsorption capacity of most adsorbents [31,32]. However, the electrostatic repulsion between anionic PFASs and a negatively charged adsorbent could be overcome by the hydrophobic effect of the C-F chain [33]. Therefore, the removal of short-chain PFASs was mainly dependent on the electrostatic effect, while long-chain PFASs mainly tended to hydrophobic effects. Adsorption mechanisms of carbon-based adsorbents for PFASs removal are shown in Figure 1.

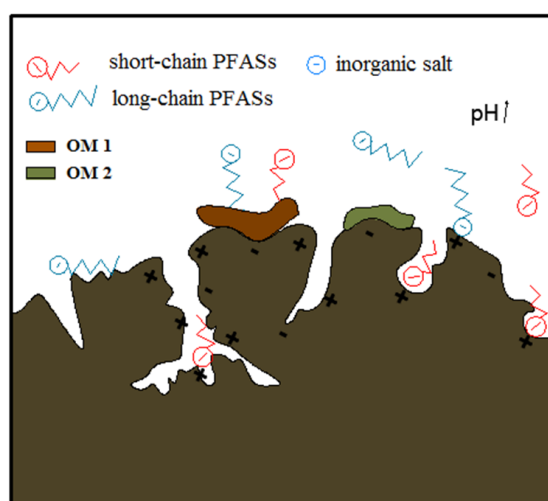
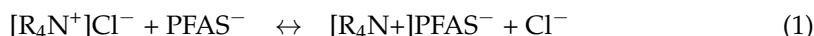


Figure 1. Adsorption mechanism of carbon-based adsorbents for PFAS removal.

3.1.2. Anion-Exchange Resin Adsorption

Resin adsorption gradually attracted researchers' attention due to its strong adsorption, regeneration ability, and convenient operation. The carbon chain length (or hydrophobicity) and terminal functional groups of PFASs could influence the adsorption of anion-exchange resin for PFASs. Maimaiti et al. explored the adsorption of large pore anion-exchange resins about IRA910 for single PFASs (PFBA, PFHxA, PFOA, PFBS, PFHxS, and PFOS), showing that the chain length had a great influence on PFCAs adsorption compared with PFSAs [34]. The adsorption efficiency of PFSAs was better than PFCAs, in which the optimum adsorption efficiency of PFBS could be up to 1023.32 mg/g. Moreover, in order to investigate the treatment effect and regeneration capacity of anion-exchange resin, Du et al. eluted the IRA67 resin that saturated adsorption with PFOA and PFHxA using the mixture solution of NaCl and methanol, the recovery could achieve 98% and 40%, respectively. This phenomenon indicated that short-chain PFASs were difficult to remove from the resin. In addition, the properties of ion-exchange resin also played an effect on the adsorption for short-chain PFASs [25]. For instance, the adsorption capacity of the ion-exchange resin was superior to the non-ion exchange resin, and most of them were better than ACs.

The mechanism of anion-exchange resin mainly included hydrophobic effects, electrostatic effects, and ion-exchange effects. Generally, the resin with stronger hydrophobicity possessed a virtuous adsorption ability; however, the regeneration capacity was deprived by contrast [4]. Furthermore, the adsorption of short-chain PFASs might be influenced by pH via changing the resin surface potential or morphology [34]. For instance, in various ranges of pH, strong base anion (SBA) resin was impregnable due to its ionization form. In contrast, weak base anion (WBA) resin was influenced significantly [31], which could take effect when the amine group was protonated under acidic conditions. Moreover, the main mechanism for short-chain PFAS removal was single-molecule anion-exchange by the analysis of transmission electron microscope; thus, the inorganic anions in solution would compete with PFAS anions for the ion-exchange sites and then decrease the removal efficiency. The ion-exchange reaction equations are shown in (1) and (2), where $[R_4N^+]$ and $[R_3N]$ indicate the ion-exchange site [15].



3.1.3. Coagulation and Electrocoagulation

Coagulation possessed the advantage of low price and high adsorption efficiency [4]. Deng et al. [35] discovered that the removal efficiency of PFOA exceeded 90% when the dosage of polymer aluminum chloride (PACl) was 10 mg/L. However, the removal efficiency of PFOA was reduced significantly when multiple PFASs existed simultaneously, and the removal rates followed the order of PFBA > PFHxA > PFOA > PFDoA > PFOS, which demonstrated that the removal efficiency of short-chain PFASs was superior, compared with long-chain congeners.

Electrocoagulation received widespread attention because of its higher removal efficiency for PFASs and short treatment period [4]. The electrocoagulation technique mainly produced a large number of cations and then generated flocs by sacrificing the anode; thus, the dissolved contaminants could be purified by condensation and adsorption of flocs, which was subsequently carried to the surface of the solution by the H_2 and O_2 produced by the electrodes through electrical floating. The Electrocoagulation mechanism for PFAS removal is shown in Figure 2. Liu et al. [36] adopted the periodically reversing electrocoagulation (PREC) technique to treat contaminated groundwater around fluorochemical plants, indicating that the PREC was effective for the removal of PFASs with different lengths of carbon chains. Subsequently, the above group approved that the PREC technique with Al-Zn electrodes for multiple PFSA removal was impactful, the removal rates of PFBS, PFHxS, and PFOS could reach up to 87.4%, 95.6%, and 100% within 10 min under

optimal conditions (12.0 V, pH = 7, 400 r/min) [37]. In general, the removal mechanism of electrocoagulation was a hydrophobic effect and might exist with electrophoretic, polarized, and electric fields [38]. In addition, several influencing factors involving current density, inorganic ions, and OM were also crucial for the removal of short-chain PFASs.

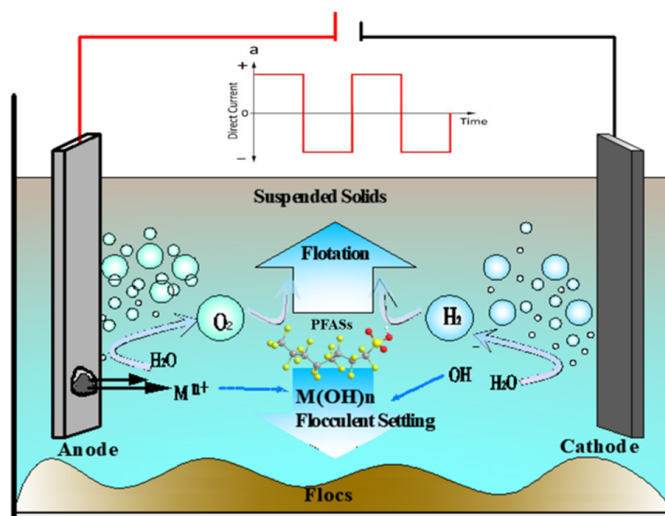


Figure 2. Electrocoagulation Mechanism for PFASs removal.

Table 2. Comparisons on adsorption capacities of various adsorbents for short-chain PFASs.

Adsorbent	Adsorbent Dose/(mg/L)	PFASs	PFAS Concentration (mg/L)	Experiment Condition	Removal Efficiency	References
GAC (F400)	1000	PFBS	15–150	DI, 30 °C, pH = 7.2	98.7 mg/g	[23]
BdAC	200	PFHxA	31.4	WW, 25 °C pH = 4, 48 h 170 r/min	18.84 mg/g	[25]
IRA67	100	PFHxA	31.4	WW, 25 °C pH = 4, 48 h 170 r/min	37.68 mg/g	[25]
AC (micropore)	250	PFBA	6.5–204	DI, room temperature	51.36 ± 4.28 mg/g	[26]
		PFBS	6–247	pH = 6, 3 d	51.01 ± 3 mg/g	
		PFHxA	7.2–217		235.54 ± 72.23 mg/g	
CTF	250	PFBA	6.5–204	DI, room temperature pH = 6, 3 d	92.03 ± 4.28 mg/g	[26]
SWCNT	250	PFBA	106.4	DI, 25 °C pH = 7, 2 d 200 r/min	7.5%	[30]
IRA910	100	PFBS	50–400	DI, 25 °C, pH = 6, 240 h 160 r/min	1023.32 mg/g	[34]
		PFBA			635.69 mg/g	
Electrocoagulation	–	PFBS	0.031	GW, pH = 7.0 10 min, 400 r/min Al-Zn, 12 V	87.4%	[36]

3.1.4. Adsorption with Other Materials

In recent years, the performance and construction of new materials that could be controlled and modified easily were synthesized by researchers. Wang et al. used a covalent triazine-based framework (CTF) to eliminate PFBS, with an adsorption capacity of 92.03 mg/g [25]. Subsequently, Zaggia et al. explored the adsorption capacity of AC, CTF, and IRA910 for PFBA and found that the order followed the rules of micropore AC < CTF < IRA910, which demonstrated the adsorption mechanism was an electrostatic effect between the triazine group and the PFAS anion head [32]. Ionic strength might be another major factor of other materials that influenced the adsorption efficiency. For example, the adsorption efficiency of poly-styrene carboxylic acid (PS-COOH) for short-chain PFCAs in seawater was better than river water due to the large ionic strength in seawater [39].

Therefore, in various kinds of adsorption materials, the adsorption efficiency of anion exchange resin and electrocoagulation for short-chain PFASs were remarkable. However, the elution ability of the anion exchange resin was inferior when the short-chain PFASs were adsorbed, and the flocs of electrocoagulation were still required for further treatment. Secondly, AC owned the property of low cost and high removal efficiency, while the regeneration ability was unsatisfactory. Finally, new adsorption materials could improve electrostatic attraction effectively, but the application should be further explored.

3.2. Advanced Oxidation/Reduction Techniques

Advanced oxidation/reduction techniques have been used for the degradation of PFASs, with the advantages of high conversion efficiency and simple operation, and some techniques could achieve complete mineralization. However, these techniques generally put emphasis on long-chain PFASs, including PFOA and PFOS. Whether these techniques could remove short-chain PFASs was still lacking in studies. This section provides a systematic summary of the application of the degradation of short-chain PFASs about the techniques of electrochemical oxidation and photocatalytic degradation, etc.

3.2.1. Electrochemical Oxidation

Electrochemical oxidation is an emerging advanced oxidation technique due to the advantages of high removal efficiency, strong oxidative ability, and low energy consumption. This technique was found to degrade long-chain PFASs effectively. The most commonly used oxidation anodes included Ti/SnO₂, Ce/PbO₂, boron-doped diamond (BDD) electrodes, and their modified electrodes. Comparisons on the removal efficiency of short-chain PFASs by different electrode materials are shown in Table 3.

Table 3. Removal efficiency of short-chain PFASs by different electrode materials.

Anode	PFASs	PFASs Concentration (mg/L)	Experiment Condition	Removal Efficiency/(%)	References
Ti/SnO ₂ -Sb/PbO ₂ -Ce	PFBA	100	20 mA/cm ² , 10 mmol/L NaClO ₄	31.8	[40]
	PPPeA			41.4	
	PFHxA			78.2	
	PFHpA			97.9	
BDD	PFHxA	870	100 mA/cm ² , OM, inorganic salt	98	[41]
Si/BDD	PFBS	>150	rotating disk electrode	90	[42]

Niu et al.'s research group found that the degradation efficiency of Ti/SnO₂-Sb for 100 mg/L PFOA could reach 98.8% when the current density was 40 mA/cm², pH at 5, and the electrolyte with 10 mmol/L NaClO₄ [43]. Subsequently, the research group explored

the Ti/SnO₂-Sb/PbO₂-Ce electrode to degrade short-chain PFASs of PFHpA and PFBA, with removal rates of 97.9% and 31.8%, respectively. This might be related to the high resistance of short-chain PFASs and the co-existence of multiple PFASs [40]. In addition, Soriano et al. used a BDD electrode to remove high concentrations of 870 mg/L PFHxA in a solution containing OM and inorganic salt, finding that the removal rate was 98% within 2 h when the current density was at 100 mA/cm², and energy consumption was 45 Wh/L [41]. Liao et al. explored a Si/BDD electrode for the elimination of high concentration PFBS (>150 mg/L) at low current density; the removal rate was 90% within 1 h [42]. Based upon the above studies, the BDD and its modified electrodes achieved remarkable results compared with other electrodes involving SnO₂ and PbO₂. However, the base materials of Si were too weak and performed unfortunate electrical conductivity. Therefore, high manufacturing costs and lack of suitable base materials limited the large-scale application of BDD electrodes. At present, it is important to discover a cheap and stable base material for the industrial application of BDD electrodes [37].

The degradation of PFASs on the electrode surface was related to electron transfer and free radical oxidation; the proposed pathways for electrochemical oxidation of PFOS in water are shown in Figure 3.

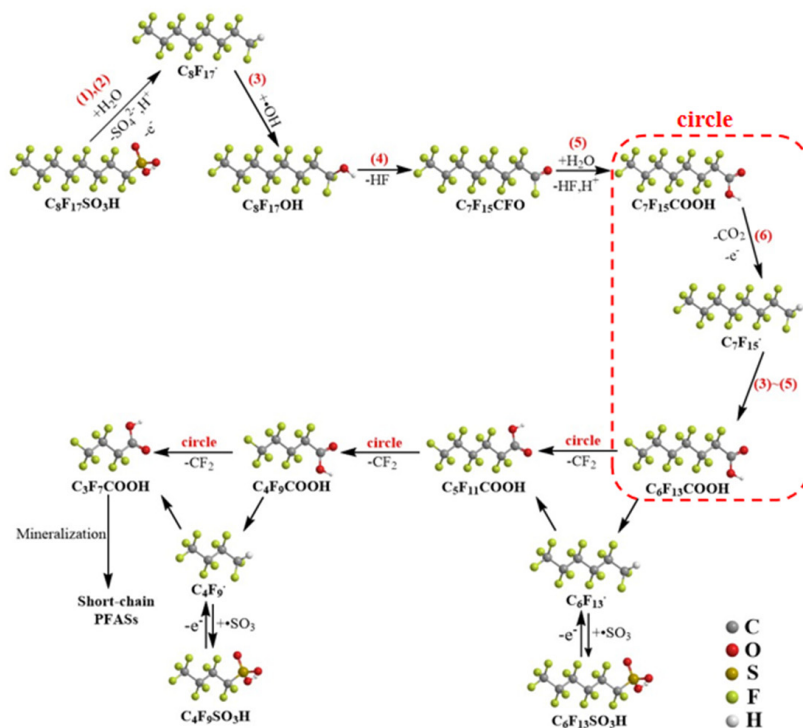
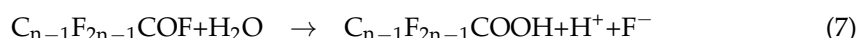


Figure 3. Proposed pathways for electrochemical oxidation of PFOS in water.

Initially, the electrons are transferred from the terminal functional group of PFASs to the anode driven by the electric field and formed PFAS radicals ($\cdot\text{C}_n\text{F}_{2n+1}\text{COO}$ or $\cdot\text{C}_n\text{F}_{2n+1}\text{SO}_3$), the extremely unstable PFAS radicals undergo decarboxylation or desulfation to form $\cdot\text{C}_n\text{F}_{2n+1}$. The generated $\cdot\text{C}_n\text{F}_{2n+1}$ could react with H_2O , OH^- , or $\cdot\text{OH}$, and finally $-\text{CF}_2$ groups were cut down gradually to generate short-chain PFASs with the specific reaction equations shown in (3)–(7) [44,45].





Plenty of studies have demonstrated that the degradation efficiency of short-chain PFASs was still lower than long-chain congeners. In order to improve the removal efficiency of short-chain PFASs and reduce the energy consumption effectively, the studies of influence factors, including the current density, pH, electrolyte, OM, and microorganisms in solution, must be carried out. Meanwhile, the electrode modification could improve the removal efficiency and the defluoridation efficiency of PFASs, as well as improve the electrode life successfully, but the metal doping on electrodes might lead to partial contamination during treatment processes [4].

3.2.2. Photocatalytic Degradation

Direct photolysis. Photocatalytic degradation is an advanced oxidation technique that can mineralize target compounds by UV light and photocatalysts. However, PFASs cannot absorb light over 220 nm directly, and the degradation rate of PFBA and PFPeA was only 16.3% and 24.3% by direct photolysis, respectively [15]. Hori et al. found that PFPeA could strongly absorb the light from the vacuum UV region to 220 nm due to the degradation of PFASs under VUV irradiation (<190 nm) by the active substances produced by homolysis and ionization of water, involving a hydrated electron (e_{aq}^-), hydrogen radical ($\text{H}\cdot$), and hydroxyl radical ($\cdot\text{OH}$) [46]. Therefore, how to use catalysts to promote the generation of active substances about free radicals for the photodegradation of PFASs was imperative. The photocatalytic efficiency of PFASs with different catalysts is shown in Table 4.

The sulfate radical ($\text{SO}_4^{\bullet-}$) produced from persulfate ($\text{S}_2\text{O}_8^{2-}$) under UV irradiation was observed to be more effective for PFASs degradation over $\cdot\text{OH}$. Therefore, $\text{S}_2\text{O}_8^{2-}$ was used as an oxidant to degrade PFAS frequently [47]. For instance, Hori et al. found that the short-chain PFCAs in aqueous solution were oxidized to CO_2 and F^- by $\text{SO}_4^{\bullet-}$ when the concentration of $\text{S}_2\text{O}_8^{2-}$ was 50 mmol/L [46]. Subsequently, this group also found that Fe^{3+} was an effective catalyst for photodegradation, and the photodegradation efficiency of PFBA and PFPeA were improved to 49.9% and 64.5% due to strong light absorption from the complexation of PFASs with Fe^{3+} [47]. Water-soluble polyacid photocatalysts could also promote C-F bond cleavage of PFPrA, thereafter generated to TFA, CO_2 , and F^- , but the energy consumption of the process was exorbitant [48].

Zero-valent iron (ZVI) reduction. Reductants including zero-valent iron particles or iodine salt could also enhance the photodegradation of PFASs. ZVI was used as a reductive agent for the photodegradation of PFASs due to its high reduction potential (-0.447 V) and reactive surface area [15]. For instance, Hori et al. observed that the degradation efficiency of short-chain PFSAs (C2-C6) could be up to 95% using ZVI, owing to the generation of iron oxide in the ZVI surface, which could interact with PFASs ions synergistically, thus promoting defluoridation efficiently [49].

Photocatalytic degradation. Photocatalysts were scarcely implemented in short-chain PFASs; the photodegradation efficiency could be deduced by examining the degradation intermediates and degradation efficiency of long-chain PFASs. For example, Panchangam et al. adopted TiO_2 photocatalysts for 120 mmol/L of PFOA degradation under UV irradiation at 254 nm within 7 h, 97% of PFOA were converted to short-chain intermediates, including PFPrA, PFBA, PFPeA, PFHxA, and PFHpA, in which PFHpA reached the maximum at 5 h [50]. Currently, the widely used method for modifying TiO_2 was doping with precious metals (Pt, Pd, Au) or other metals (Pb, Cu, Fe). Li et al. explored TiO_2 doped with Pt to completely decompose 144.9 mmol/L PFOA within 7 h under UV irradiation at 365 nm; the defluoridation efficiency was 34.8%. It was 12.5-fold faster than unmodified TiO_2 due to the deposited Pt particles could store excessive electrons and promote the electrons transferred to PFAS available [51]. In addition, the composite materials were used to improve the photocatalytic degradation of PFASs, such as TiO_2 -MWCNT and TiO_2 -rGO. It was found that the degradation efficiency of PFOA could reach 100% when using TiO_2 -MWCNT after 8 h under irradiation of UV at 265 nm [52].

In addition to the above n-type photocatalysts of TiO_2 , p-type photocatalysts involving In_2O_3 and Ga_2O_3 have attracted widespread attention because they could enhance the degradation capacity of PFASs. However, p-type photocatalysts showed a strong dependence on the material shape and microstructure [15]. For example, the In_2O_3 porous microsphere had the highest photocatalytic activity on the degradation of PFOA, which was 74.7 times faster than TiO_2 . Similarly, short-chain intermediate PFHpA could be completely degraded within 3 h by the In_2O_3 nanoplates, whereas In_2O_3 nanocubes were much less effective. However, in the degradation process, the short-chain intermediates were still generated from PFOA degradation, and the concentration of intermediates was positively related to their carbon chain length [50,53].

New photocatalysts could decompose PFAS, but the information about the application for short-chain PFASs was still limited. According to the degradation data of long-chain PFASs, the degradation conclusions could be deduced as the following: photocatalytic degradation of PFASs was a gradual splitting decomposition of CF_2 . The reaction of breaking the chain generated short-chain intermediates. The short-chain products showed strong resistance to photocatalytic degradation [15].

During the photodegradation process, the catalyst dosage and pH were imperative influencing factors. In the low concentration range between 20–100 mmol/L of persulfate, the photochemical reactivity could be improved with the concentration increase. Whereas further increasing persulfate concentrations could result in saturation of the reaction rate. Because $\text{SO}_4^{\bullet-}$ could react with persulfate or itself, this side reaction would reduce the degradation efficiency [15]. Moreover, a high concentration of hydrated hydrogen ions (H_3O^+) would quench e_{aq}^- under acidic conditions, thus contributing to the reactivity decrease due to the quantum yield of e_{aq}^- declining sharply. However, under alkaline conditions, the reactivity would be enhanced due to the quantum yield of e_{aq}^- increasing by the reaction of $\text{H}\cdot$ and OH^- [54].

Table 4. Photocatalytic efficiency of PFASs with different catalysts.

Catalyst	Catalyst Dose	PFASs	Experiment Condition	Removal Efficiency (%)	References
Fe^{3+}	5 mmol/L	PFBA PFPeA	UV UV	49.9 64.5	[47]
ZVI particles	960 mmol/L	Short-chain PFASs (C2–C6)	UV, 350 °C 20 MPa	95	[49]
TiO_2	0.66 g/L	PFOA	254 nm $\text{pH} < 3$	100%	[50]
TiO_2 -MWCNT	0.4 g/L	PFOA	300 W, 365 nm $\text{pH} = 5$	100%	[52]
TiO_2 -rGO	0.1 g/L	PFOA	150 W, 254 nm $\text{pH} = 3.8$	93 ± 7%	[55]

3.3. Other Techniques

3.3.1. Plasma Technique

Plasma is the collection of positive and negative electric particles that consist of electrons, ions, radicals, and neutral particles, which are electric and electroneutral, thus called the fourth state beyond gas, liquid, and solid electrically. Diverse from most AOPs and conventional techniques, plasma techniques could convert water into highly active substances, involving $\cdot\text{OH}$, O_\cdot , $\text{H}\cdot$, $\text{HO}_2\cdot$, $\text{O}_2^{\bullet-}$, H_2 , O_2 , H_2O_2 , and e_{aq}^- [56]. When using the plasma technique for PFASs elimination, the degradation process was gradually reduced to intermediates, and then intermediates, perfluoroalkyl radicals, and perfluoro alcohols/ketones-perfluoroalkyl were oxidized [57]. However, this technique was hardly

applied and is invalid in the degradation for short-chain PFASs. For example, Takaki et al. adopted BaTiO₃ iron beads as a filling medium to degrade C₂F₆; the degradation efficiency was only 20% [58]. Moreover, short-chain PFASs, fluorine ions, and CO₂ by-products were produced during the plasma treatment of PFASs.

3.3.2. Thermolytic and Sonochemical Degradation

In the recent decade, thermolytic and sonochemical degradation have attracted wide attention. Tsang et al. [59] found that 99% of CF₄ could be removed under urban incineration conditions (about 850 °C) and assumed the pyrolysis of 800–900 °C could resolve long and short-chain PFASs efficiently. Krusic et al. [60] explored the gas phase decomposition of PFOA in quartz tubes at 355–385 °C, finding that PFOA retained thermal stability below 300 °C but completely degraded at 370 °C after 360 min. However, the by-products of small molecule substances were generated continuously, which demonstrated the greater resistance of short-chain PFASs. Subsequently, Campbell et al. explored pre-concentrating PFHxA on GAC, which could improve the thermal mineralization rate from 46% to 74% [61]. Furthermore, in order to investigate the effect of ultrasonic chemistry on the degradation of PFASs with different carbon chain lengths, Campbell et al. investigated the degradation efficiency on six kinds of PFASs at 358 kHz, the order was PFOA > PFHxA > PFBA and PFOS ≈ PFHxS > PFBS [62]. Similarly, Fernandez et al. found that the degradation efficiency of ultrasonic chemicals raised with carbon chain length increased [63]. For one thing, long-chain PFASs with strong hydrophobicity were inclined to be adsorbed on the gas-liquid interface for thermal decomposition or oxidation degradation. For another, short-chain PFASs were more difficult to be defluorinated than long-chain congeners. Generally, these techniques could mineralize short-chain PFASs, but nongreen environmental factors about the generous discharge of CO₂ and high energy consumption limited the development in actual application.

3.3.3. Membrane Separation

In recent years, low carbon treatment of membrane separation techniques, including nanofiltration (NF) and reverse osmosis (RO), have made great advances. During the rejection in membrane processes, the molecular size and structure of PFASs were considered key factors. For instance, NF membranes could reject more than 96% of PFHxA ($\mu\text{g/L}$ to mg/L) under neutral pH, whereas the rejection rate of shorter-chains PFASs about PFBS decreased to 69% attributable to the small molecular size [64]. Furthermore, charge, hydrophobicity, pH, and dipole moment might also affect the solute-membrane interactions and thus the rejection efficiency of PFAS. It was shown that pH reduction could increase the membrane rejection efficiency of PFHxA. Moreover, the presence of the ions generally suppressed the electrical repulsion, but the exclusion efficiency was enhanced with increasing ionic strength, which indicated that the exclusion of membrane size was the dominant factor. In the practical application, the rejection efficiency of short-chain PFASs would be easily influenced because of membrane contamination. In addition, membrane separation techniques could produce a high concentration of PFASs and still require subsequent treatment or disposal.

3.3.4. Bioremediation Techniques

Kwon et al. degraded PFOS (1400–1800 $\mu\text{g/L}$) by cultivating *P. aeruginosa* microorganism with the removal rate of 67% [65]. However, short-chain PFASs were difficult to degrade by common microbes. For example, the concentration of PFBS in the effluent of sewage treatment plants remained unchanged or increased after conventional activated sludge or biofilm bioreactors. That is, short-chain PFASs showed high resistance to various activated sludge systems [5]. While in plant tissues, both short and long-chain PFASs all have a tendency to accumulate. Recent studies have shown that the biological accumulation of PFASs followed a U-type trend. The lowest hydrophobicity (e.g., PFBA and PFPeA) and the maximum hydrophobic species (e.g., PFNA and PFDA) presented the greatest absorb-

efficiency [66]. Another study on the uptake and distribution of PFASs in maize showed that plant adsorption and distribution of PFASs were dependent on chain length, functional groups, and plant tissue. Generally, short-chain PFASs were transferred to the overground portion of plants, while long-chain PFASs were mainly transported to the root [67].

4. Comparisons on Different Treatment Techniques

So far, low carbon treatment techniques of short-chain PFASs have included adsorption, membrane separation, bioremediation, as well as degradation techniques relating to advanced oxidation, plasma, thermolytic, and sonochemical degradation. The above technologies could remove short-chain PFASs to a certain extent, but their treatment effects, operating conditions, removal mechanism, and applicability were quite different. The comparisons on treatment techniques for short-chain PFASs are presented in Table 5.

Adsorption was the utmost widely applied technique for short-chain PFASs, and its energy consumption could be nearly ignored besides the low energy cost of the adsorbent regeneration. The removal mechanisms of short-chain PFASs were mainly electrostatic action, hydrophobic effect, and ion exchange [4]. As shown in Table 5, this technique has the advantages of convenient operation, low carbon, low cost, and low energy consumption, as well as application with a wide concentration range of short-chain PFASs, especially trace levels. However, the technique has the drawbacks of a long adsorption period and low regeneration efficiency [27,36].

Advanced oxidation techniques, involving electrochemical oxidation and photocatalytic degradation, degraded short-chain PFASs primarily relying on active free radicals, which possessed the advantages of a short treatment period and low energy consumption [5,15]. However, the techniques were not suitable for trace levels of short-chain PFASs, and its low mineralization rate and subsequent CO₂ generation rate from mineralization were also the main problems for achieving the low-carbon goals [43]. In addition, electrochemical oxidation could produce high expenses of electrode materials and the risk of electrode contamination. The photocatalytic degradation technique generated the problem of secondary pollution by catalyst addition and might thus be limited in actual applications [15].

The plasma technique was applied to the degradation of long-chain PFASs effectively, but few studies focused on its degradation of short-chain PFASs, and the energy consumption was still higher for complete mineralization [58]. The thermolytic and sonochemical techniques could achieve complete mineralization, but the energy consumption was too high, and the operating conditions were stringent [61]. The membrane separation technique could reject short-chain PFAS pollutants effectively, but membrane pollution and membrane flux instability were the main problems [64]. Bioremediation techniques could take advantage of their low carbon and environmentally-friendly processes, but they generated the problems of long remediation period and low efficiency, as well as inefficient short-chain PFAS elimination and remaining in organisms [65].

Based upon the analysis, the most widely used and effective method could be adsorption, followed by advanced oxidation. However, there were still limitations of removal efficiency in the application of eliminating short-chain PFASs. Since short-chain PFASs were more resistant to be adsorbed and degraded than long-chain congeners, PFASs of C1–C3 were barely degradable. Combined techniques might be developed based on concentration/recycling-degradation of short-chain PFASs in water bodies rather than degradation. The combination of adsorption and gas–liquid series electrical discharge treatment has been applied in the degradation of dyestuff, which achieved excellent removal efficiency compared with the adsorption alone [68].

Table 5. Comparisons on treatment techniques for short-chain PFASs.

Technique	Materials	Advantage	Disadvantage	Removal Mechanism	Treatment Time	Removal Efficiency	Energy Consumption	References
Adsorption	ACs, Anion-exchange resin	Low carbon, cost, energy consumption, and convenient operation; No change in physicochemical properties; Wide concentrations and trace short-chain PFASs could be treated.	Long adsorption time and unfortunate regeneration capacity of sorbent; Secondary contamination of elution solvent.	Electrostatic interaction; Hydrophobic interaction; Ion exchange	10 min–10 d	10–95.6%	—	[25,27,36]
Electrochemical oxidation	Ti/SnO ₂ , BDD	Low energy consumption and short time; Good treatment for short-chain PFASs.	Expensive electrode materials; Not suitable for trace contamination; Prone to secondary contamination and produced intermediates.	Oxidation; Hydrophobic interaction	1–3 h	31.8–98%	45 Wh/L	[40,43]
Photocatalytic degradation	UV, S ₂ O ₈ ²⁻ Fe ³⁺ , ZVI	Mineralizable.	Additional catalyst; Low degradation efficiency; Complex by-products.	Oxidation; Reduction.	6 h–10 d	16–95%	29–9091 Wh/L	[15,69,70]
Plasma	Grinding nickel chrome rod	Short time; Suitable for long-chain PFASs.	High energy consumption; Low mineralization efficiency; Generate intermediates.	Reduction.	1–2 h	20%	—	[57,58]
Thermolytic and sonochemical degradation	High temperature; Ultrasonic	Fully mineralized.	Long time; High energy consumption.	Disrupts molecular structure by high energy	6–65 h	46–74%	2129 Wh/L	[60,61]
Membrane separation	NF RO	Low carbon and energy consumption; Better rejection of short-chain PFASs.	Not suitable for the actual waters; Easy to occur in membrane pollution.	Rejection	—	69–96%	—	[64]
Bioremediation	Corn	Low carbon and environmentally-friendly; Effective to some degree for some short-chain PFASs by plant adsorption.	Long time and ineffective.; Need targeted training.	—	>2 d	~67%	—	[65]

5. Conclusions and Future Research Recommended

This paper showed that the adsorption, electrochemical oxidation, and photocatalytic degradation have certain removal effects on short-chain PFASs by comparisons on various treatment techniques. Considering the removal efficiency, treatment time, energy consumption, and cost, adsorption was the most widely applied technique for the effective removal of short-chain PFASs, which was suitable for a wide concentration range of pollution and to meet the low-carbon policy. Whereas, long adsorption period and unsatisfied regeneration ability were the main problems. The advanced oxidation techniques of electrochemical and photocatalytic activity could degrade short-chain PFASs, but low mineralization efficiency contributed to intermediates of short-chain PFASs, as well as abundant organic matter and CO₂ and they were especially inappropriate to eliminate trace short-chain PFASs. Therefore, it was desirable to choose suitable techniques according to PFAS properties, as well as the advantages and disadvantages of various techniques.

The contaminations of short-chain PFASs have attracted much attention at present, while most studies still focused on the laboratory-scale treatment of long-chain PFASs, including PFOA and PFOS, and data on the treatment of short-chain PFASs is still absent. Therefore, future studies need to focus on the following topics: (1) Targeting long duration period and poor material regeneration ability for the adsorption technique; the functional groups of adsorbent materials need to be modified for improving electrostatic attraction and hydrophobic effects and enhancing the adsorption efficiency and elution of short-chain PFASs. (2) Innovative design for short-chain PFAS treatment by electrode and catalyst modification to develop advanced oxidation techniques, with high degradation efficiency in low-carbon and low-energy consumption, as well as adaptability for low-concentration PFASs. (3) With the increasing pollution of short-chain PFASs in drinking water, extensive emphasis should be placed on the development of advanced treatment techniques for actual groundwater and surface water, along with exploration of new adsorption materials, electrode materials, and catalysts, which could remove low concentrations of short-chain PFAS under the background of multiple substances co-existing in the actual waters. (4) Short-chain PFASs were more resistant to degradation than long-chain congeners, and PFASs of C1-C3 were barely degradable. Therefore, concentration/recycling of short-chain PFASs in water bodies should be considered rather than degradation. In addition, combined techniques might be developed based on concentration/recycling-degradation, such as adsorption and advanced oxidation, for the efficient removal of short-chain PFASs from actual waters.

Author Contributions: Conceptualization, Y.L. and J.B.; methodology, Y.L. and T.L.; software, M.L.; validation, X.Z., C.L. and L.S.; formal analysis, T.L.; investigation, T.L.; resources, Y.L. and J.B.; data curation, T.L. and X.H.; writing—original draft preparation, Y.L. and J.B.; writing—review and editing, Y.L. and X.H.; visualization, T.L.; supervision, Y.L. and T.L.; project administration, Y.L. and J.B.; funding acquisition, J.B. All authors have read and agreed to the published version of the manuscript.

Funding: This research was funded by the National Natural Science Foundation of China (No. 21976124 and No. 21507092), the Natural Science Foundation of Liaoning Province of China (No. 2019-ZD-0217), and the Liaoning Revitalization Talents Program (No. XLYC2007195).

Acknowledgments: Thanks for the financial support from the National Natural Science Foundation of China (No. 21976124 and No. 21507092), the Natural Science Foundation of Liaoning Province of China (No. 2019-ZD-0217), and the Liaoning Revitalization Talents Program (No. XLYC2007195).

Conflicts of Interest: The authors declare no conflict of interest.

References

- Rahman, M.F.; Peldszus, S.; Anderson, W.B. Behaviour and fate of perfluoroalkyl and polyfluoroalkyl substances (PFASs) in drinking water treatment: A review. *Water Res.* **2013**, *50*, 318–340. [[CrossRef](#)] [[PubMed](#)]
- Jian, J.; Chen, D.; Han, F.; Guo, Y.; Zeng, L.; Lu, X.; Wang, F. A short review on human exposure to and tissue distribution of per- and polyfluoroalkyl substances (PFASs). *Sci. Total Environ.* **2018**, *636*, 1058–1069. [[CrossRef](#)] [[PubMed](#)]
- Park, M.; Wu, S.; Lopez, I.J.; Chang, J.Y.; Karanfil, T.; Snyder, S.A. Adsorption of perfluoroalkyl substances (PFAS) in groundwater by granular activated carbons: Roles of hydrophobicity of PFAS and carbon characteristics. *Water Res.* **2020**, *170*, 115364. [[CrossRef](#)] [[PubMed](#)]
- Liu, Y.; Hu, X.; Zhao, Y.; Wang, J.; Bao, J. Treatment techniques for perfluorinated compounds and their alternatives. *Environ. Chem.* **2018**, *37*, 1860–1868. [[CrossRef](#)]
- Ateia, M.; Maroli, A.; Tharayil, N.; Karanfil, T. The overlooked short- and ultrashort-chain poly- and perfluorinated substances: A review. *Chemosphere* **2019**, *220*, 866–882. [[CrossRef](#)] [[PubMed](#)]
- Reemtsma, T.; Berger, U.; Arp, H.P.H.; Gallard, H.; Knepper, T.P.; Neumann, M.; Quintana, J.B.; Voogt, P.D. Mind the gap: Persistent and mobile organic compounds-water contaminants that slip through. *Environ. Sci. Technol.* **2016**, *50*, 10308–10315. [[CrossRef](#)]
- Arp, H.P.H.; Brown, T.N.; Berger, U.; Hale, S.E. Ranking REACH registered neutral, ionizable and ionic organic chemicals based on their aquatic persistency and mobility. *Environ. Sci.-Proc. Imp.* **2017**, *19*, 939–955. [[CrossRef](#)]
- Kotthoff, M.; Bücking, M. Four Chemical trends will shape the next decade's directions in perfluoroalkyl and polyfluoroalkyl substances research. *Front. Chem.* **2018**, *6*, 1–6. [[CrossRef](#)]
- Gellrich, V.; Stahl, T.; Knepper, T.P. Behavior of perfluorinated compounds in soils during leaching experiments. *Chemosphere* **2012**, *87*, 1052–1056. [[CrossRef](#)]
- Brendel, S.; Fetter, É.; Staude, C.; Vierke, L.; Biegel-Engler, A. Short-chain perfluoroalkyl acids: Environmental concerns and a regulatory strategy under REACH. *Environ. Sci. Eur.* **2018**, *30*, 9. [[CrossRef](#)]
- Zhou, Z.; Liang, Y.; Shi, Y.; Xu, L.; Cai, Y. Occurrence and transport of perfluoroalkyl acids (PFAAs), including short-chain PFAAs in Tangxun Lake, China. *Environ. Sci. Technol.* **2013**, *47*, 9249–9257. [[CrossRef](#)] [[PubMed](#)]
- Bao, J.; Li, C.; Liu, Y.; Wang, X.; Yu, W.; Liu, Z.; Shao, L.; Jin, Y. Bioaccumulation of perfluoroalkyl substances in greenhouse vegetables with long-term groundwater irrigation near fluorochemical plants in Fuxin, China. *Environ. Res.* **2020**, *188*, 109751. [[CrossRef](#)] [[PubMed](#)]
- Eschauzier, C.; Beerendonk, E.; Scholte-Veenendaal, P.; Voogt, P.D. Impact of treatment processes on the removal of perfluoroalkyl acids from the drinking water production chain. *Environ. Sci. Technol.* **2012**, *46*, 1708–1715. [[CrossRef](#)] [[PubMed](#)]
- Schmidt, C.K.; Brauch, H.J. N, N-dimethylsulfamide as precursor for N-nitrosodimethylamine (NDMA) formation upon ozonation and its fate during drinking water treatment. *Environ. Sci. Technol.* **2008**, *42*, 6340–6346. [[CrossRef](#)] [[PubMed](#)]
- Li, F.; Duan, J.; Tian, S.; Ji, H.; Zhu, Y.; Wei, Z.; Zhao, D. Short-chain per- and polyfluoroalkyl substances in aquatic systems: Occurrence, impacts and treatment. *Chem. Eng. J.* **2020**, *380*, 122506. [[CrossRef](#)]
- Wang, H.; Lu, X.; Deng, Y.; Sun, Y.; Nielsen, C.P.; Liu, Y.; Zhu, G.; Bu, M.; Bi, J.; McElroy, M. China's CO₂ peak before 2030 implied from characteristics and growth of cities. *Nat. Sustain.* **2019**, *2*, 748–754. [[CrossRef](#)]
- Watts, M. Commentary: Cities spearhead climate action. *Nat. Clim. Chang.* **2017**, *7*, 537–538. [[CrossRef](#)]
- Wang, Y.; Xu, Z.; Zhang, Y. Influencing factors and combined scenario prediction of carbon emission peaks in megacities in China: Based on Threshold-STIRPAT model. *Acta Sci. Circumst.* **2019**, *39*, 4284–4292. [[CrossRef](#)]
- Song, Q.; Liu, T.; Qi, Y. Policy innovation in low carbon pilot cities: Lessons learned from China. *Urban Clim.* **2021**, *39*, 100936. [[CrossRef](#)]
- Liu, Q.; Zhang, W.; Yao, M.; Yuan, J. Carbon emissions performance regulation for China's top generation groups by 2020: Too challenging to realize? *Resour. Conserv. Recy.* **2017**, *122*, 326–334. [[CrossRef](#)]
- Ma, W.; De, J.M.; De, B.M.; Mu, R. Mix and match: Configuring different types of policy instruments to develop successful low carbon cities in China. *J. Clean. Prod.* **2021**, *282*, 125399. [[CrossRef](#)]
- Glüge, J.; Scheringer, M.; Cousins, I.T.; DeWitt, J.C.; Goldenman, G.; Herzke, D.; Lohmann, R.; Ng, C.A.; Trier, X.; Wang, Z. An overview of the uses of per- and polyfluoroalkyl substances (PFAS). *Environ. Sci. Process Impacts* **2020**, *22*, 2345–2373. [[CrossRef](#)] [[PubMed](#)]
- Ochoa-Herrera, V.; Sierra-Alvarez, R. Removal of perfluorinated surfactants by sorption on to granular activated carbon, zeolite and sludge. *Chemosphere* **2008**, *72*, 1588–1593. [[CrossRef](#)] [[PubMed](#)]
- Hansen, M.C.; Borresen, M.H.; Schlabach, M.; Cornelissen, G. Sorption of perfluorinated compounds from contaminated water to activated carbon. *J. Soils Sediments* **2010**, *10*, 179–185. [[CrossRef](#)]
- Du, Z.; Deng, S.; Chen, Y.; Wang, B.; Huang, J.; Wang, Y.; Yu, G. Removal of perfluorinated carboxylates from washing wastewater of perfluorooctanesulfonate fluoride using activated carbons and resins. *J. Hazard. Mater.* **2015**, *286*, 136–143. [[CrossRef](#)] [[PubMed](#)]
- Wang, B.; Lee, L.S.; Wei, C.; Fu, H.; Zheng, S.; Xu, Z.; Zhu, D. Covalent triazine-based framework: A promising adsorbent for removal of perfluoroalkyl acids from aqueous solution. *Environ. Pollut.* **2016**, *216*, 884–892. [[CrossRef](#)]
- McCleaf, P.; Englund, S.; Östlund, A.; Lindegren, K.; Wiberg, K.; Ahrens, L. Removal efficiency of multiple poly- and perfluoroalkyl substances (PFASs) in drinking water using granular activated carbon (GAC) and anion exchange (AE) column tests. *Water Res.* **2017**, *120*, 77–87. [[CrossRef](#)]

28. Wang, M.; Zhou, Q. Environmental effects and their mechanisms of biochar applied to soils. *Environ. Chem.* **2013**, *32*, 768–780. [[CrossRef](#)]
29. Inyang, M.; Dickenson, E.R.V. The use of carbon adsorbents for the removal of perfluoroalkyl acids from potable reuse systems. *Chemosphere* **2017**, *184*, 168–175. [[CrossRef](#)]
30. Deng, S.; Zhang, Q.; Nie, Y.; Wei, H.; Wang, B.; Huang, J.; Yu, G.; Xing, B. Sorption mechanisms of perfluorinated compounds on carbon nanotubes. *Environ. Pollut.* **2012**, *168*, 138–144. [[CrossRef](#)]
31. Gagliano, E.; Sgroi, M.; Falciglia, P.P.; Vagliasindi, F.G.A.; Roccaro, P. Removal of poly- and perfluoroalkyl substances (PFAS) from water by adsorption: Role of PFAS chain length, effect of organic matter and challenges in adsorbent regeneration. *Water Res.* **2020**, *171*, 115381. [[CrossRef](#)] [[PubMed](#)]
32. Gao, Y.; Deng, S.; Du, Z.; Liu, K.; Yu, G. Adsorptive removal of emerging polyfluoroalkyl substances F-53B and PFOS by anion-exchange resin: A comparative study. *J. Hazard. Mater.* **2017**, *323*, 550–557. [[CrossRef](#)] [[PubMed](#)]
33. Zaggia, A.; Conte, L.; Falletti, L.; Fant, M.; Chiorboli, A. Use of strong anion exchange resins for the removal of perfluoroalkylated substances from contaminated drinking water in batch and continuous pilot plants. *Water Res.* **2016**, *91*, 137–146. [[CrossRef](#)] [[PubMed](#)]
34. Maimaiti, A.; Deng, S.; Meng, P.; Wang, W.; Wang, B.; Huang, J.; Wang, Y.; Yu, G. Competitive adsorption of perfluoroalkyl substances on anion exchange resins in simulated AFFF-impacted groundwater. *Chem. Eng. J.* **2018**, *348*, 494–502. [[CrossRef](#)]
35. Deng, S.; Zhou, Q.; Yu, G.; Huang, J.; Fan, Q. Removal of perfluorooctanoate from surface water by polyaluminium chloride coagulation. *Water Res.* **2011**, *45*, 1774–1780. [[CrossRef](#)]
36. Liu, Y.; Hu, X.; Zhao, Y.; Wang, J.; Lu, M.; Peng, F.; Bao, J. Removal of perfluorooctanoic acid in simulated and natural waters with different electrode materials by electrocoagulation. *Chemosphere* **2018**, *201*, 303–309. [[CrossRef](#)]
37. Bao, J.; Yu, W.; Liu, Y.; Wang, X.; Liu, Z.; Duan, Y. Removal of perfluoroalkanesulfonic acids (PFSAs) from synthetic and natural groundwater by electrocoagulation. *Chemosphere* **2020**, *248*, 125951. [[CrossRef](#)]
38. Niu, J.; Wang, C.; Shang, E. Removal of perfluorinated compounds from wastewaters by electrochemical methods: A general review. *Sci. Sin. Technol.* **2017**, *47*, 1233–1255. [[CrossRef](#)]
39. Llorca, M.; Schirinzi, G.; Martínez, M.; Barceló, D.; Farré, M. Adsorption of perfluoroalkyl substances on microplastics under environmental conditions. *Environ. Pollut.* **2018**, *235*, 680–691. [[CrossRef](#)]
40. Niu, J.; Lin, H.; Xu, J.; Wu, H.; Li, Y. Electrochemical mineralization of per-fluorocarboxylic acids (PFCAs) by Ce-doped modified porous nanocrystalline PbO₂ film electrode. *Environ. Sci. Technol.* **2012**, *46*, 10191–10198. [[CrossRef](#)]
41. Soriano, A.; Gorri, D.; Urtiaga, A. Efficient treatment of perfluorohexanoic acid by nanofiltration followed by electrochemical degradation of the NF concentrate. *Water Res.* **2017**, *112*, 147–156. [[CrossRef](#)] [[PubMed](#)]
42. Liao, Z.; Farrell, J. Electrochemical oxidation of perfluorobutane sulfonate using borondoped diamond film electrodes. *J. Appl. Electrochem.* **2009**, *39*, 1993–1999. [[CrossRef](#)]
43. Niu, J.; Li, Y.; Shang, E.; Xu, Z.; Liu, J. Electrochemical oxidation of perfluorinated compounds in water. *Chemosphere* **2016**, *146*, 526–538. [[CrossRef](#)] [[PubMed](#)]
44. Lin, H.; Niu, J.; Liang, S.; Wang, C.; Wang, C.; Wang, Y.; Jin, F.; Luo, Q.; Chiang, S.Y.D.; Huang, Q. Development of macroporous magneli phase Ti₄O₇ ceramic materials: As an efficient anode for mineralization of poly- and perfluoroalkyl substances. *Chem. Eng. J.* **2018**, *354*, 1058–1067. [[CrossRef](#)]
45. Niu, J.; Lin, H.; Gong, C.; Sun, X. Theoretical and experimental insights into the electrochemical mineralization mechanism of perfluorooctanoic acid. *Environ. Sci. Technol.* **2013**, *47*, 14341–14349. [[CrossRef](#)]
46. Hori, H.; Yamamoto, A.; Hayakawa, E.; Taniyasu, S.; Yamashita, N.; Kutsuna, S.; Kiatagawa, H.; Arakawa, R. Efficient decomposition of environmentally persistent perfluorocarboxylic acids by use of persulfate as a photochemical oxidant. *Environ. Sci. Technol.* **2005**, *39*, 2383–2388. [[CrossRef](#)]
47. Hori, H.; Yamamoto, A.; Koike, K.; Kutsuna, S.; Osaka, I.; Arakawa, R. Photochemical decomposition of environmentally persistent short-chain perfluorocarboxylic acids in water mediated by iron (II)/(III) redox reactions. *Chemosphere* **2007**, *68*, 572–578. [[CrossRef](#)]
48. Hori, H.; Takano, Y.; Koike, K.; Kutsuna, S.; Einaga, H.; Ibusuki, T. Photochemical decomposition of pentafluoropropionic acid to fluoride ions with a water-soluble heteropolyacid photocatalyst. *Appl. Catal. B-Environ.* **2003**, *46*, 333–340. [[CrossRef](#)]
49. Hori, H.; Nagaoka, Y.; Yamamoto, A.; Sano, T.; Yamashita, N.; Taniyasu, S.; Kutsuna, S.; Osaka, I.; Arakawa, R. Efficient decomposition of environmentally persistent perfluorooctanesulfonate and related fluorochemicals using zerovalent iron in subcritical water. *Environ. Sci. Technol.* **2006**, *40*, 1049–1054. [[CrossRef](#)]
50. Panchangam, S.C.; Lin, A.; Shaik, K.L.; Lin, C. Decomposition of perfluorocarboxylic acids (PFCAs) by heterogeneous photocatalysis in acidic aqueous medium. *Chemosphere* **2009**, *77*, 242–248. [[CrossRef](#)]
51. Li, M.; Yu, Z.; Liu, Q.; Sun, L. Photocatalytic decomposition of per-fluorooctanoic acid by noble metallic nanoparticles modified TiO₂. *Chem. Eng. J.* **2016**, *286*, 232–238. [[CrossRef](#)]
52. Song, C.; Chen, P.; Wang, C.; Zhu, L. Photodegradation of perfluorooctanoic acid by synthesized TiO₂–MWCNT composites under 365nm UV irradiation. *Chemosphere* **2011**, *86*, 853–859. [[CrossRef](#)] [[PubMed](#)]
53. Chen, M.; Lo, S.L.; Lee, Y.C.; Huang, C.C. Photocatalytic decomposition of perfluorooctanoic acid by transition-metal modified titanium dioxide. *J. Hazard. Mater.* **2015**, *288*, 168–175. [[CrossRef](#)] [[PubMed](#)]

54. Jin, L.; Zhang, P. Photochemical decomposition of perfluorooctane sulfonate (PFOS) in an anoxic alkaline solution by 185nm vacuum ultraviolet. *Chem. Eng. J.* **2015**, *280*, 241–247. [[CrossRef](#)]
55. Gomez-Ruiz, B.; Ribao, P.; Diban, N.; Rivero, M.J.; Ortiz, I.; Urtiaga, A. Photocatalytic degradation and mineralization of perfluorooctanoic acid (PFOA) using a composite TiO₂-rGO catalyst. *J. Hazard. Mater.* **2017**, *344*, 950–957. [[CrossRef](#)]
56. Stratton, G.R.; Dai, F.; Bellona, C.L.; Holsen, T.M.; Dickenson, E.R.V.; Thagard, S.M. Plasma-Based water treatment: Efficient transformation of perfluoroalkyl substances in prepared solutions and contaminated groundwater. *Environ. Sci. Technol.* **2017**, *51*, 1643–1648. [[CrossRef](#)]
57. Singh, R.K.; Fernando, S.; Baygi, S.F.; Multari, N.; Thagard, S.M.; Holsen, T.M. Breakdown products from perfluorinated alkyl substances (PFAS) degradation in a plasma-based water treatment process. *Environ. Sci. Technol.* **2019**, *53*, 2731–2738. [[CrossRef](#)]
58. Takaki, K.; Urashima, K.; Chang, J.S. Scale-up of ferro-electric packed bed reactor for C₂F₆ decomposition. *Thin Solid Films* **2006**, *506*, 414–417. [[CrossRef](#)]
59. Tsang, W.; Burgess, D.R.; Babushok, V. On the Incinerability of Highly Fluorinated Organic Compounds. *Combust. Sci. Technol.* **1998**, *139*, 385–402. [[CrossRef](#)]
60. Krusic, P.J.; Roe, D.C. Gas-phase NMR studies of the thermolysis of perfluorooctanoic acid. *Anal. Chem.* **2005**, *126*, 1510–1516. [[CrossRef](#)]
61. Watanabe, N.; Takata, M.; Takemine, S.; Yamamoto, K. Thermal mineralization behavior of PFOA, PFHxA, and PFOS during reactivation of granular activated carbon (GAC) in nitrogen atmosphere. *Environ. Sci. Pollut. Res. Int.* **2018**, *25*, 7200–7205. [[CrossRef](#)] [[PubMed](#)]
62. Campbell, T.Y.; Vecitis, C.D.; Mader, B.T.; Hoffmann, M.R. Perfluorinated surfactant chain-length effects on sonochemical kinetics. *J. Phys. Chem. A* **2009**, *113*, 9834–9842. [[CrossRef](#)] [[PubMed](#)]
63. Fernandez, N.A.; Rodriguez-Freire, L.; Keswani, M.; Sierra-Alvarez, R. Effect of chemical structure on the sonochemical degradation of perfluoroalkyl and poly-fluoroalkyl substances (PFASs). *Water Res.* **2016**, *2*, 975–983. [[CrossRef](#)]
64. Wang, J.; Wang, L.; Xu, C.; Zhi, R.; Miao, R.; Liang, T.; Yue, X.; Lv, Y.; Liu, T. Perfluorooctane sulfonate and perfluorobutane sulfonate removal from water by nanofiltration membrane: The roles of solute concentration, ionic strength, and macromolecular organic foulants. *Chem. Eng. J.* **2018**, *332*, 787–797. [[CrossRef](#)]
65. Kwon, B.G.; Lim, H.J.; Na, S.H.; Choi, B.I.; Shin, D.S.; Chung, S.Y. Biodegradation of perfluorooctanesulfonate (PFOS) as an emerging contaminant. *Chemosphere* **2014**, *109*, 221–225. [[CrossRef](#)] [[PubMed](#)]
66. Müller, C.E.; LeFevre, G.H.; Timofte, A.E.; Hussain, F.A.; Sattely, E.S.; Luthy, R.G. Competing mechanisms for perfluoroalkyl acid accumulation in plants revealed using an arabidopsis model system. *Environ. Toxicol. Chem.* **2016**, *35*, 1138–1147. [[CrossRef](#)] [[PubMed](#)]
67. Krippner, J.; Brunn, H.; Falk, S.; Georgii, S.; Schubert, S.; Stahl, T. Effects of chain length and pH on the uptake and distribution of perfluoroalkyl substances in maize (*Zea mays*). *Chemosphere* **2014**, *94*, 85–90. [[CrossRef](#)]
68. Zhang, Y.Z.; Zheng, J.T.; Qu, X.F.; Chen, H.G. Effect of granular activated carbon on degradation of methyl orange when applied in combination with high-voltage pulse discharge. *J. Colloid Interface Sci.* **2007**, *316*, 523–530. [[CrossRef](#)]
69. Chen, J.; Zhang, P.; Liu, J. Photodegradation of perfluorooctanoic acid by 185 nm vacuum ultraviolet light. *J. Environ. Sci.* **2007**, *19*, 387–390. [[CrossRef](#)]
70. Hori, H.; Yamamoto, A.; Kutsuna, S. Efficient photochemical decomposition of long-chain perfluorocarboxylic acids by means of an aqueous/liquid CO₂ biphasic system. *Environ. Sci. Technol.* **2005**, *39*, 7692–7697. [[CrossRef](#)]